J. Fluid Mech. (1996), vol. 315, pp. 51–64

A comparison of numerical predictions and experimental measurements of the internal kinematics of a deep-water plunging wave

By DAVID SKYNER

Department of Mechanical Engineering, University of Edinburgh, Edinburgh EH9 3JL, UK

(Received 26 September 1994 and in revised form 5 October)

A deep-water long-crested breaking wave is generated from a time-stepping numerical model, then replicated in a wave flume. The numerical model is based on the boundary integral method and measurements of the internal kinematics are made during the breaking process with Particle Image Velocimetry (PIV). Velocity measurements are obtained throughout the wave crest, including the plunging spout. After a small shift of the numerical data to match the surface profiles, the predicted and measured kinematics are found to be in good agreement, within the limits of experimental error.

1. Introduction

Breaking waves represent some of the most extreme events in the marine environment. Their internal kinematics have implications for the safety of ships, the design of oil platforms and the processes of coastal erosion. Many studies on such waves have been performed, particularly those breaking on beaches, which have been reviewed by Peregrine (1983). In deep water, recent research effort by Kjeldsen (1990) and Sand *et al.* (1990) has been applied to the assessment of the probability of freak waves occurring, as well as by Kjeldsen (1980) to the mechanics of the breaking.

The breaking process is difficult to measure and to model. Nevertheless, good quantitative descriptions of the breaking process have been reported by Basco (1985), Miller (1976) and Tallent, Yamashita & Tsuchiya (1990). Recently, measurements have been made of the crest kinematics just before breaking by Griffiths, Easson & Greated (1992), of the aeration induced by the breaking process by Lamarre & Melville (1991), and of the turbulence left afterwards by Nakagawa (1991).

Numerical computations of the evolution of overturning waves were first performed by Longuet-Higgins & Cokelet (1976). Since then refinements have been made, and a number of robust, fully nonlinear time-stepping numerical models have become available for two-dimensional water waves (Dold & Peregrine 1986; Grilli & Svendsen 1990; She, Greated & Easson 1992). However, they can be difficult to apply to practical situations and in their application are limited to the early stages of breaking. A good review of numerical computations is given by Peregrine (1990).

Experimental studies have been undertaken for comparison with numerical predictions, most notably by Dommermuth *et al.* (1988). Here, good agreement was obtained between point measurements of the internal kinematics and the prediction of a numerical model, for a deep-water breaking wave. However, the velocity measurements were not made in the breaking crest, but a few metres closer to the wavemaker and mainly below the still-water level. It was found that the nonlinear computations

predict that the wave plunges closer to the wavemaker and at an earlier time than is observed, with deviations in position and time of $\Delta x \approx 0.15$ m and $\Delta t \approx 0.25$ s. Comparative studies such as this are rare, perhaps because of the difficulties encountered in trying to arrange the same experimental and numerical conditions.

In the present study, a particular deep-water, plunging, breaking wave was chosen and investigated in great detail. The wave selected was arbitrary, but it was considered more important that similar waves could be generated numerically and experimentally, than that the chosen wave should have any particular parameters, other than being extreme. The study concentrates on extracting as much information as possible about the kinematics of this particular wave using the Particle Image Velocimetry (PIV) measurement technique, and on the careful comparison between the measurements and the numerical predictions. In making velocity measurements throughout the whole of the breaking crest, the study goes significantly beyond that of Dommermuth *et al.* (1988). The design of the wave flume built for the project allowed the same wave to be followed through all phases of its evolution, from its initial steepening, until after breaking. The work consolidates and expands upon earlier work of the author (Skyner & Greated 1992; Skyner, Gray & Greated 1990).

The numerical model used in the study was a time-stepping program written at the University of Bristol by Dold & Peregrine (1986), based on the boundary integral method with assumptions of inviscid, incompressible and irrotational flow. In the model, computational points are positioned along the surface boundary, each with a coordinate and velocity potential. The computational points are given starting values and are allowed to move. Cauchy's integral theorem is used to solve Laplace's equation for the time derivatives of the surface motion. The surface points are propagated until a specified time, or until the calculations become unstable if the wave is overturning. An important feature of the numerical scheme is the use of higher-order derivatives in the time-stepping, resulting in a computationally efficient scheme. It is implicit in the formulation that the end boundary conditions are periodic.

PIV (Adrian 1984; Pickering & Halliwell 1984) is a reliable measurement technique which can yield very accurate, simultaneous velocity measurements over a wide area of a flow field. In PIV, multiple images of small tracer particles are recorded onto film which is subsequently analysed to determine the particle motions and hence the velocity field. Since the early experiments by Barker & Fourney (1977), Grousson & Mallick (1977) and Simpkins & Dudderar (1978), the PIV method has received much research attention, aided by the increased availability of high-powered lasers to illuminate the flow and the advance in the speed of computers, making automated analysis of the photographs possible. A good review of the technique has been given by Gray (1992). While the principles of the method are well established in general, each application requires particular implementations and practices (Greated, Skyner & Bruce). For the study of the kinematics of water waves, PIV has only recently been developed (Gray 1989), and is now at the stage where it can be used to yield reliable velocity measurements, as discussed by Quinn *et al.* (1992), Skyner & Greated (1992) and Sutherland, Greated & Easson (1991).

2. Generation of the extreme wave

In the numerical model, starting values for the computational points along the surface are required, whereas in the wave flume, the motion of the wave paddle is specified as a function of time. In order to ensure that similar waves are generated in

the model and flume, it is necessary to obtain one set of boundary conditions from the other, and it was found to be easier to specify the numerical conditions first.

2.1. *Generation of the extreme wave in the numerical model*

The approach used to generate the breaking wave in the time-stepping numerical model was similar to that adopted in the laboratory to produce an extreme wave for demonstration purposes: linear theory was used to force an extreme event, then the parameters of the generation were modified slowly until a suitable plunging wave resulted.

Each attempt at producing a numerical breaker followed the same pattern. First, parameters for a chosen spectrum were selected. Next the surface profile and velocity potential were calculated by linear superposition using using equation (2.1), with ω_n and k_n related by the linear dispersion relationship. These quantities were appropriately scaled for the model, and care was taken to ensure that the wave packets tailed off smoothly before the periodic boundaries. The distribution of computational points was also forced to be smooth across the boundary. The numerical wave group was then allowed to propagate until it 'broke' or passed the point where breaking was expected. Depending on the result from the run, the spectral parameters were altered until a plunging breaker was produced which just avoided breaking at the penultimate crest. The main parameter to be modified was the overall size of the spectrum.

$$A(x,t) = \mathrm{Re}\left\{\sum_{n=N_0}^{N_1} A_n \mathrm{e}^{-\mathrm{i}(k_n x+\omega_n t+\alpha_n)}\right\}. \tag{2.1}$$

In order to limit the number of parameters the spectral shape was selected such that the components had amplitudes given by

$$A_n = (a_0 + a_1\omega_n)\exp\left(-\left|\frac{\omega-\Omega_1}{\Omega_0}\right|^S\right) \tag{2.2}$$

where

$$\omega_n = \frac{2\pi n}{102.4}. \tag{2.3}$$

The phases α_n were chosen so that, if linear theory applied, the components would have some common phase $\Phi = 0$ at $x = 0, t = 0$.

The spectral form given in (2.2) was selected as covering the 'flat top' spectral shape often used in the generation of freak waves by, for example, Dommermuth *et al.* (1988) and Greenhow *et al.* (1982), while allowing the spectrum to tail off smoothly at the extremes. Initial parameters were chosen with a knowledge of the dimensions and capabilities of the wave flume.

With 200 computational points it was possible to try another iteration every few hours, and after less than 30 iterations a suitable breaker was arrived at. The chosen wave was then rerun with twice the number of computational points. The profile of the wave as it nears breaking, used to judge its suitability, is plotted in figure 1.

The spectral shape which yielded this final profile is plotted in figure 2 and the spectral parameters noted in table 1. The spectrum shown is somewhat different from those naturally occurring in the oceans, where normally the wave component amplitude tails off with frequency above the central value. When the wave packet reaches the wave flume, its spectral form has been modified by nonlinear action to one which is more usual in shape, as can be seen by looking forward to figure 7. For

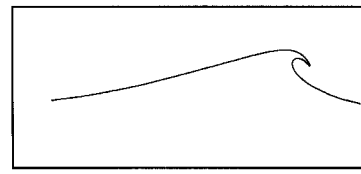

FIGURE 1. Final surface profile as the numerical wave approaches breaking.

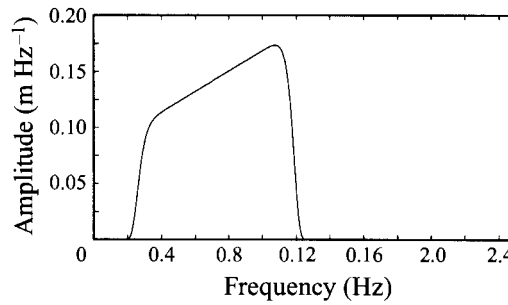

FIGURE 2. Wave amplitude spectrum found to produce a suitable numerical breaker.

Parameter	Value
a_0	0.75498 mm
a_1	1.4161 mm s rad^{-1}
Ω_0	2.93230 rad s^{-1}
Ω_1	4.53174 rad s^{-1}
s	16

TABLE 1. Parameters selected for the spectrum used to calculate the starting conditions for the numerical model

the purpose of non-dimensionalizing the results, the mean frequency of the spectrum has been calculated as $f_m = 0.818$ Hz, with corresponding wavelength $\lambda_m = 2.26$ m. In the work of Dommermuth *et al.* (1988) the central frequency of the spectrum was 0.88 Hz.

The starting conditions for the numerical model calculated from this spectrum are plotted, at tank scale, in figure 3 along with the distribution function used to obtain the coordinates of the computational points. The distribution function peaks near the place where breaking is expected, in order that there are enough points where the surface curvature is the highest and the greatest accuracy is required. Note that the horizontal extent of the starting conditions is about five times longer than the actual wave flume, which starts at $x' = -3.8$ m in this figure.

2.2. *Strategy for matching the waves*

From the data produced by the numerical model it is possible to extract any physical information about the wave packet as it propagates from the starting conditions until the program halts at the breaking point. While it would be possible to calculate a wave time-series to be produced at the wavemaker, this is not practical as the travelling wave at this position is distorted by the evanescent effects of the wave paddle (Hyun 1976). A better strategy is to obtain a wave height time-series from

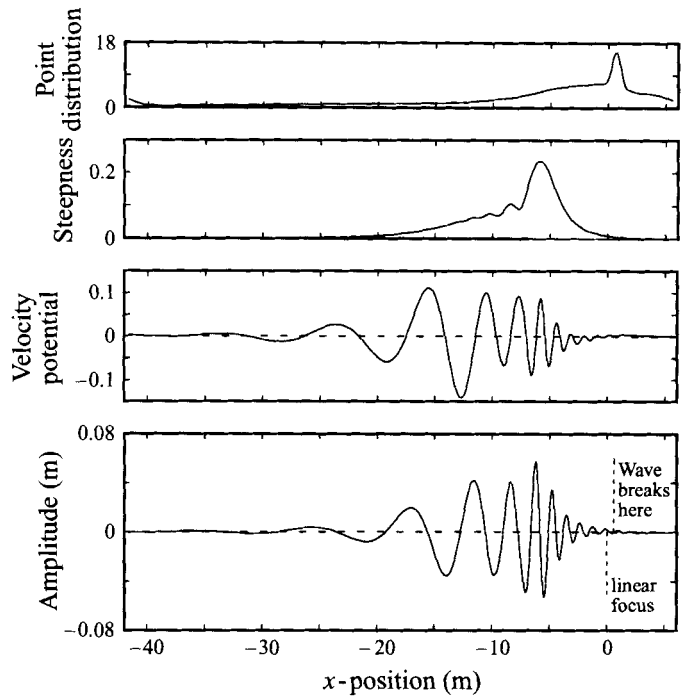

FIGURE 3. Starting profile and velocity potential calculated by linear theory 7.3 s before expected linear focus.

the model and to attempt to reproduce this in the flume far enough in front of the wavemaker to avoid transient effects.

The position for the wave gauge in the numerical wave tank was selected to be at $x = -1.6$ m, which is about 2 m before the final breaking position. By interpolating between the records at the neighbouring computational points a wave height time-series was extracted from the numerical data. The equivalent position in the physical wave flume was selected to be at $x' = 2.2$ m, from considerations of the part of the flume where PIV measurements of the breaking kinematics would be easiest to make.

The criterion for success in the replication is that the wave height time-series should match well at the selected wave gauge position. The approach adopted was to form the amplitude and phase spectrum of the numerical time-series and to attempt to reproduce this in the tank. Because the waves are markedly nonlinear at the selected position, the linear wavemaker transfer function cannot be expected to produce the required record directly, and an iterative scheme was attempted.

In forming the spectrum of the numerical time-series a difficulty is encountered: only part of the time-series exists, from the chosen start until wave breaking. The time-series was extended outside this range by calculation with linear theory from the starting spectrum. The composite time-series obtained in this way is shown in figure 4. The linear focus was arranged to be at 12.071 s on this scale.

2.3. *Generation of the extreme wave in the wave flume*

Figure 5 shows the configuration of the wave flume for the experimental replication of the numerical wave, including the position of the wave gauge. Also shown are the actual wave profiles obtained in the experiments and the physical coordinate system,

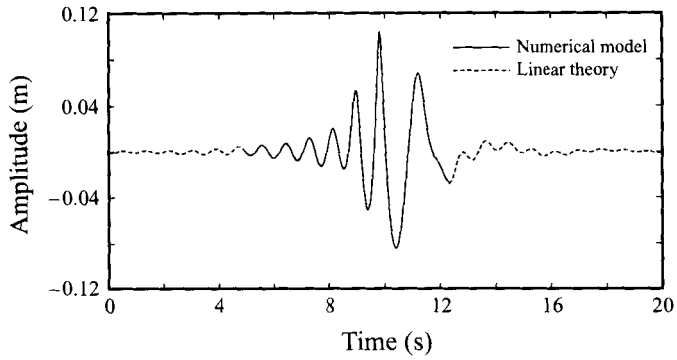

FIGURE 4. Composite wave amplitude time-series from the numerical model and linear theory.

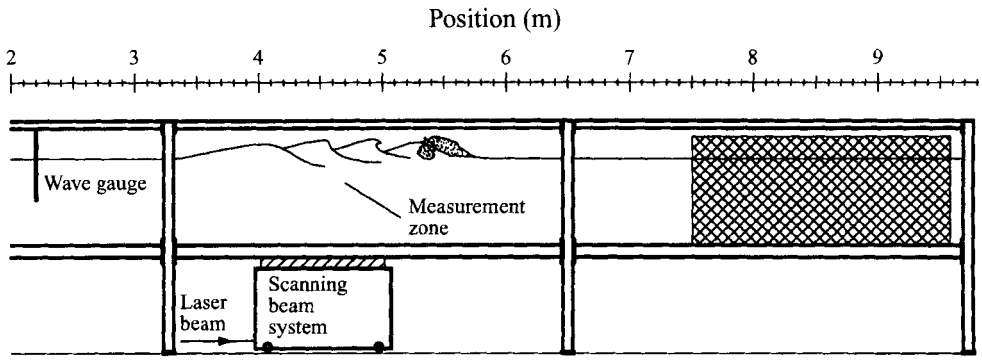

FIGURE 5. Configuration of the wave flume for the measurement of breaking waves.

which is related to the numerical coordinate system by $x' = x + 3.8$ m. Waves are generated by a hinged-paddle absorbing wavemaker described by Salter (1982), travel from left to right, and are absorbed by a mesh beach at the end of the flume. The illumination system which provides the pulsed light sheet for the PIV photography is mounted on rails and can be moved anywhere beneath the two first measurement bays. The flume is 9.770 m long and 0.400 m wide. The normal water depth is 0.750 m; x is measured along the flume from the wavemaker, and z upwards from the water surface.

The parameters involved in attempting to reproduce the required wave spectrum are the frequency limits of the wavemaker drive spectrum, f_1 and f_2, and the position of the wave gauge. In addition there are the details of the iterative scheme and the number of iterations involved.

The initial wavemaker drive spectrum was calculated from the linear transfer function and tried in the flume. The wave gauge was sampled as the wave group passed. The later portion of the wave record, after the breaking, contains reflections and spurious high frequencies from the wavemaker's final large motion which are difficult to disentangle in a nonlinear wave field. Therefore, the experimental wave record was patched with the linearly expected time-series used to extend the numerical record. In this way, the same operations were performed on both the numerical and experimental wave time-series before transformation. The required and obtained spectra were then compared. If the match was judged inadequate, then each component in

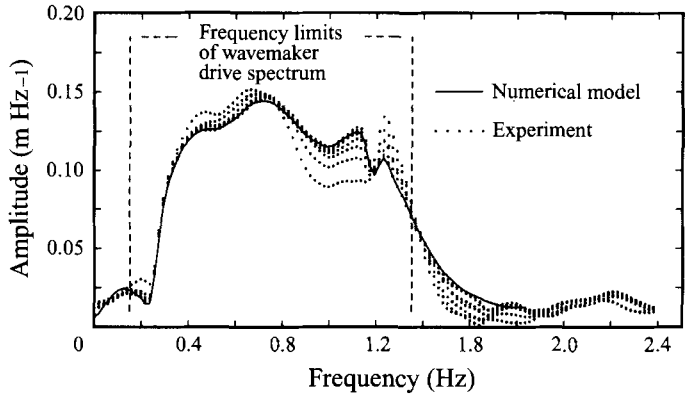

FIGURE 6. Iterations towards the required wave amplitude spectrum.

the drive spectrum was modified in both amplitude and phase by multiplication by the complex quantity $R(\omega)$ given by

$$R(\omega) = \left(\frac{A(\omega)_{required}}{A(\omega)_{obtained}} \right)^{1/2}. \tag{2.4}$$

This modifier has the effect of stepping halfway to that required in both amplitude and phase and was used because the simple ratio was found to overshoot.

Iterations were continued until the obtained spectrum was judged to match that required sufficiently closely. In the iterations, the lower frequencies were found to converge first, which is expected because the higher frequencies are partially composed of their harmonics. This can be seen in figure 6 which shows the convergence of the experimental wave spectrum to that required over six iterations.

Contained in figure 7 are the amplitude and phase of the experimental wave spectrum finally achieved, compared to the required spectrum. The spectra can be seen to have been forced to be very similar within the frequency range for which waves were generated. Below the lower frequency limit, there is also good agreement, both in amplitude and phase. This portion of the spectrum corresponds to the bound long wave, and it is important that the spectra match in this region.

The actual wave amplitude time-series is plotted in figure 8 and is compared to the time-series extracted from the numerical model. The match is generally good in the main part of the wave group. However, there is a tendency for the largest crests to be not well replicated. It should be noted that the portion after breaking is not relevant as it has no influence on the breaking event.

The repeatability of the wave spectrum was excellent. However, it can be expected that the exact form of the breaking wave will be very sensitive to small changes in the starting conditions of its evolution. Therefore, a series of tests was conducted to attempt to discover the effect of changes in the spectrum and other conditions on the final breaking form. Changes in the frequency bounds of the generated spectrum, the number of iterations in the fitting of the spectrum, the position of the wave gauges and their calibration values were amongst those investigated. Of these parameters only changes in the higher frequency bound were found to affect the breaking form significantly.

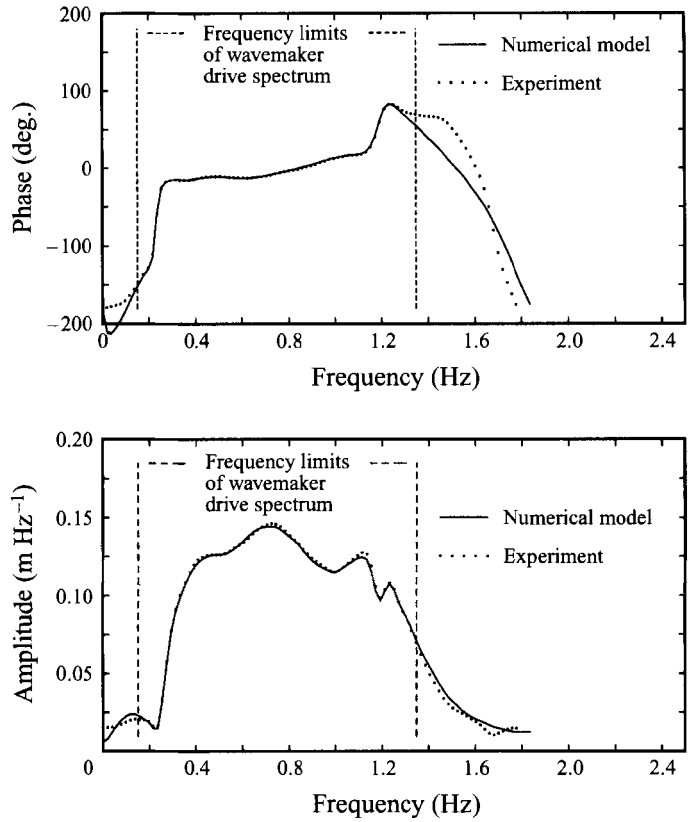

FIGURE 7. Experimental wave spectrum found by iteration compared to the required spectrum.

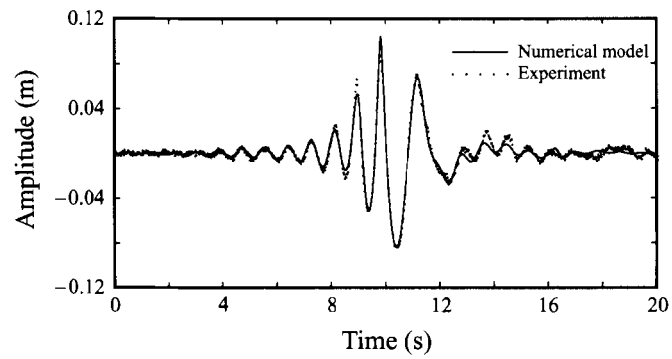

FIGURE 8. Experimental wave amplitude time-series compared to the time-series extracted from the numerical model.

3. Experimental measurements

Having established a wave group in the flume which match that in the numerical model, a sequence of measurements was performed to record the surface profiles and internal kinematics at each stage of its evolution.

The internal kinematics were obtained from PIV photographs of the flow. A Hasselblad 500 *EL/M* camera was used with an 80 mm lens and 400 ASA TMax film. The flow field was seeded with conifer pollen and illuminated with a scanning-

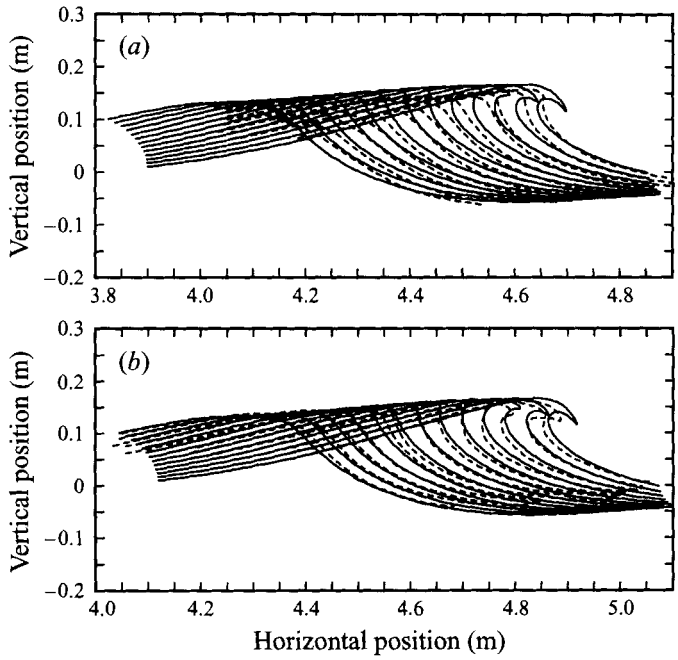

FIGURE 9. (*a*) Comparison of experimental and numerical surface profiles, from $t = 12.000$ s to $t = 12.300$ s: - - -, experimental measurements; —, numerical predictions. (*b*) As (*a*) but with shifted numerical predictions.

beam illumination system with light from a 15 W Argon-ion laser. A sequence of photographs was recorded consisting of re-runs of the breaking wave each with a given trigger time, camera position, illumination interval and shutter period. The trigger time was set by the wavemaker-controlling computer, taking account of the inherent delay of the shutter opening and half the shutter speed. Full details of the PIV experiments can be found in Skyner (1992).

3.1. *Experimental results*

Figure 9(*a*) contains the experimental and numerical surface profiles in the same graph, without any shift of the numerical results. Both sequences cover exactly the same time range at the same intervals. It can be seen that while the overall position of each phase is in close agreement with the prediction, the form of each phase is not.

While it would be preferable to compare the internal kinematics of the experimental results with predictions at the same time and place, the difference in form of such paired phases makes this ideal approach pointless. It was decided, for the purpose of the later comparison of the internal kinematics, that the numerical sequence should be considered as being shifted forward in time by 0.125 s and forward in space by 0.22 m. These shifts are similar in magnitude and of the same sign as those noted by Dommermuth *et al.* (1988). The shifted numerical surface profiles are plotted along with their corresponding experimental profiles in figure 9(*b*). While the method used for replicating the numerical wave in the tank failed to produce an exact match of the profiles near breaking, it did produce a short sequence of waves which had very similar form numerically and experimentally.

Close-up PIV measurements were taken of the plunging tip and the internal

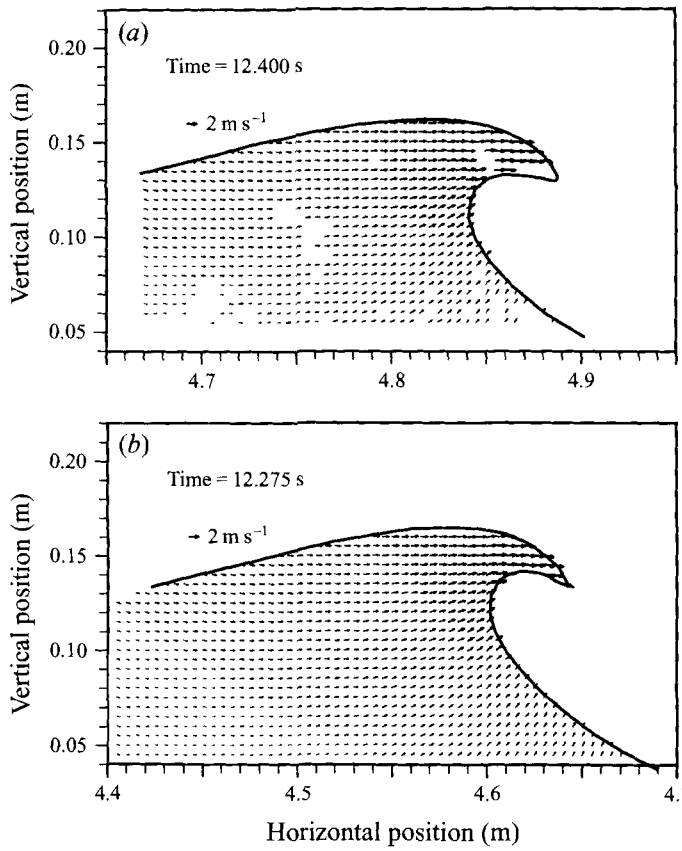

FIGURE 10. (*a*) Experimentally measured velocity field, plunging phase. (*b*) Numerically generated velocity field.

kinematics obtained are are shown in figure 10(*a*) in the form of a vector plot. It can been seen that velocity measurements are obtained in the crest, even into the plunging tip, where the illuminating beam must have passed through two water surfaces. The large patch of missing vectors in the middle of the figure is due to a registration mark on the glass obscuring the view.

In figure 10(*b*), a numerically generated velocity field is plotted for the phase matching that shown in the experimental plot, figure 10(*a*). The similarity is striking apart from the missing vectors.

To highlight the differences between the experimentally measured and numerically generated vector fields, the data were subtracted. Figure 11 shows the difference between figure 10(*a*) and figure 10(*b*). This time the numerical data have been shifted sideways by 0.24 m and upwards by 0.005 m. Note that the velocity vectors are plotted 10 times bigger than in the plots of the raw data. The difference between these shifts and those used earlier is similar to the spatial repeatability, i.e. around 0.020 m.

The overall quality of the match is very high, with many areas containing only very small vectors. However, in the region where the water surface has a vertical front there are some significant discrepancies, which is to be expected in this area of high acceleration if the vector fields are not exactly aligned.

From the maximum numerical velocity (2.3 m s^{-1}) and the mean of the magnitudes

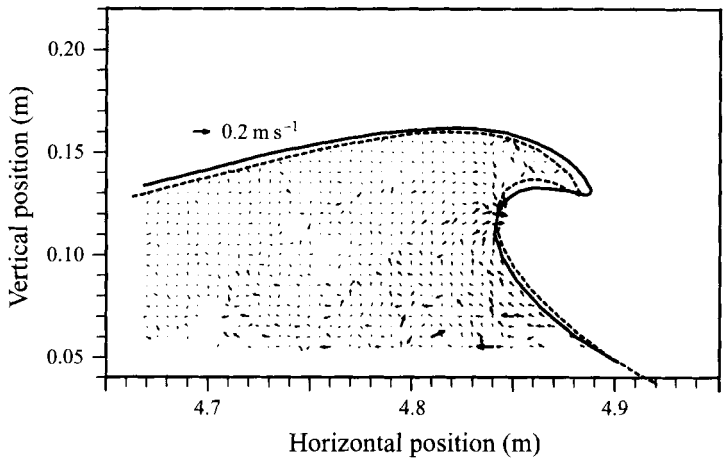

FIGURE 11. Difference between experimentally measured velocity field, $t = 12.400$ s, and numerical data, $t = 12.275$ s: —, experimental surface; - - -, numerical surface. Note the scale of the velocity vectors differs from that of figure 10.

of the subtracted velocities (0.039 m s^{-1}), the quality of the match can be estimated to be 1.7%. The standard deviation of the velocity magnitudes corresponds to 1.2%, the mean of the v_x components to 0.2% and the mean of the v_z components to 0.5%. There is no apparent systematic trend in the data and it is not clear which is the most appropriate statistic for judging the match.

In order to gauge repeatability and experimental noise, two experimental vector fields for this phase of the wave were subtracted. One of the flow fields was shifted by 0.020 m before the subtraction so that the surface profiles would match. The match appears slightly better than that between experiment and prediction, with no systematic trends near the front face of the wave. Applying the same calculations to the statistics, the mean value of the velocity magnitudes was found to be 1.1% of the maximum velocity, the mean of v_x to be 0.8% and the mean of v_z to be 0.4%.

In figure 12, the numerical data are plotted as velocity contours for the phase of the wave which can be compared to the experimental data. The most noticeable feature is a region of very high acceleration where the water surface has a vertical front (Peregrine, Cokelet & McIver 1980). Not surprisingly, this is the region where the greatest difference occurred between the numerical predictions and the experimental data plotted in figure 11.

4. Discussion

Similar waves were generated numerically and experimentally. The wave spectra shown in figure 7 match extremely well both in amplitude and phase, as does the resulting wave elevation time-series shown in figure 8. The extent of the agreement of the later phases of the wave train and possible explanations of discrepancies between the two approaches constitutes the main point of the study.

Substantial agreement is found in a number of areas. The wave crests immediately prior to breaking are at the same positions at any given time (figure 9(*a*)). For comparable wave profiles as the wave starts to plunge, the internal kinematics match within the limits of experimental repeatability and measurement error.

However, there is a notable discrepancy in the detailed form of the crests as the

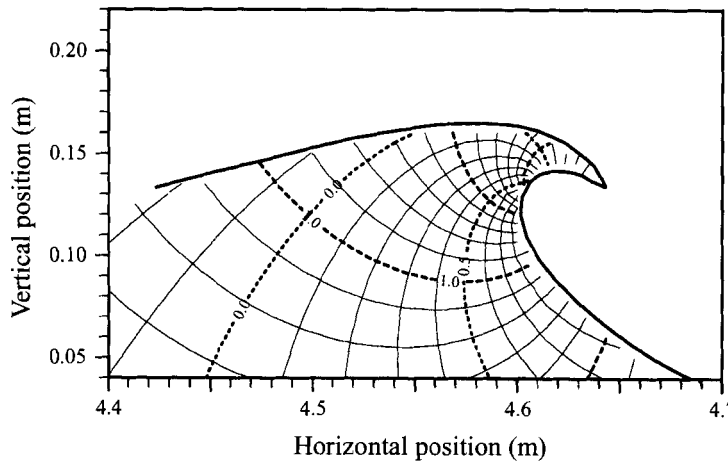

FIGURE 12. Numerical isovelocity contours, $t = 12.275$ s.

wave approaches breaking (figure 9(*a*)). This was also found in the earlier work of the author (Skyner *et al.* 1990), and has been the subject of further investigation. It is expected that breaking events are very sensitive to small differences in conditions and a number of possible contributing effects are noted:

(*a*) The wave spectra did not match perfectly in phase at high frequencies and the resulting wave elevation time-series differed slightly at the crests. Attempting to improve the match at high frequencies tended to make the wave break much too early.

(*b*) The numerical model has periodic boundary conditions which might allow a wave to travel into the measurement zone from the opposite direction. However, a check revealed that the amplitude of this wave was less than 1% of the breaking wave height. In addition, no reflections were observed in the wave flume.

(*c*) There could be effective currents in the numerical model. However, calculations yielded a value of 4 mm s^{-1} of the mean current in the model, which is negligible compared to the peak velocities of 2 m s^{-1}. No net current is expected in the flume.

(*d*) Inadequacies of the experiments were considered, including poor calibration of the wave gauges, but a sensitivity analysis did not suggest that the discrepancies were due to this.

(*e*) Other areas of possible doubt include the method of forcing the match between the numerical and the experimental spectrum and the calculation of the initial conditions for the model.

5. Conclusions

For plunging waves of similar shape, numerical predictions for the internal kinematics agreed with experimental measurements within 2%, even in the spout. The discrepancy is within the limits of experimental repeatability and measurement error.

However, the wave crests did not match perfectly on the approach to breaking. In the numerical model, the wave plunges earlier and closer to the wavemaker. No definitive explanation is offered, although the magnitude of this discrepancy is similar to that found in other work.

It is suggested that use of a numerical wave tank, configured to be as similar as

possible to the experimental facility, might reduce the number of differences between the predictions and measurements in any future work.

The author gratefully thanks Professor D. H. Peregrine and his colleagues at the School of Mathematics, University of Bristol who developed the time-stepping computer program and allowed its use at Edinburgh, Dr C. Gray who initiated the PIV studies at Edinburgh, and Professor C. A. Greated for his encouragement of the project.

REFERENCES

ADRIAN, R. J. 1984 Scattering particle characteristics and their effect on pulsed laser measurement of fluid flow: Speckle Velocimetry vrs Particle Image Velocimetry. *Appl. Optics* **23**(11), 1690–1691.

BARKER, D. B. & FOURNEY, M. E. 1977 Measuring fluid velocities with speckle patterns. *Appl. Optics* **1**(4), 135–137.

BASCO, D. R. 1985 A qualitative description of wave breaking. *J. Waterway, Port, Coastal Ocean Engng ASCE* **111**, 171–188.

DOLD, J. W. & PEREGRINE, D. H. 1986 An efficient boundary-integral method for steep unsteady water waves. In *Numerical Methods for Fluid Dynamics II* (ed. K. W. Morton & M. J. Baines), pp. 671–679. Oxford University Press.

DOMMERMUTH, D. G., YUE, D. K. P., LIN, W. M., RAPP, R. J., CHAN, E. S. & MELVILLE, W. K. 1988 Deep-water plunging breakers: a comparison between potential theory and experiments. *J. Fluid Mech.* **189**, 432–442.

GRAY, C. 1989 The development of Particle Image Velocimetry for water wave studies. PhD thesis, The University of Edinburgh.

GRAY, C. 1992 The evolution of Particle Image Velocimetry. *Optical Methods and Data Processing in Heat and Fluid Flow, City University, 2–3 April*, pp. 19–36.

GREATED, C. A., SKYNER, D. J. & BRUCE, T. 1992 Particle Image Velocimetry (PIV) in the Coastal Engineering laboratory. *Proc. 23rd Intl Conf. Coastal Engng*, pp. 212–225.

GREENHOW, M., VINJE, T., BREVIG, P. & TAYLOR, J. 1982 A theoretical and experimental study of the capsize of Salter's Duck in extreme waves. *J. Fluid Mech.* **118**, 221–239.

GRIFFITHS, M. W. P., EASSON, W. J. & GREATED, C. A. 1992 Measured internal kinematics for shoaling waves with theoretical comparisons. *J. Waterway, Port, Coastal, Ocean Engng, ASCE* **118**, 280–299.

GRILLI, S. & SVENDSEN, I. A. 1990 Computation of nonlinear wave kinematics during propagation and runup on a slope. In *Water Wave Kinematics* (ed. A. Torum & O. T. Gudmestad), pp. 387–412. Kluwer.

GROUSSON, R. & MALLICK, S. 1977. Study of the flow pattern in a fluid by scattered laser light. *Appl. Optics* **16**, 2334–2336.

HYUN, J. M. 1976 Theory for hinged wavemakers of finite draft in water of constant depth. *J. Hydronautics* **10**, 2–7.

KJELDSEN, S. P. 1980. 2- and 3-dimensional deterministics freak waves. *NHL Trondheim Norway, Pub.* R-149.83.

KJELDSEN, S. P. 1990 Breaking waves. In *Water Wave Kinematics* (ed. A. Torum & O. T Gudmestad), pp. 453–473. Kluwer.

LAMARRE, E. & MELVILLE, W. K. 1991 Air entrainment and dissipation in breaking waves. *Nature* **351**, 469–472.

LONGUET-HIGGINS, M. S. & COKELET, E. D. 1976 The deformation of steep surface waves in water. A numerical method of computation. *Proc. R. Soc. Lond.* A **350**, 1–26.

MILLER, R. L. 1976 The role of vorticies in surf zone prediction: sedimentation and wave forces. *Soc. Econ. Paleontol. Mineral.*, Special Pub. **24**, 92–114.

NAKAGAWA, T. 1991 On measurements of the water-particle velocity under breaking waves over the horizontal step in a laboratory tank. *Intl J. Offshore Polar Engng* **1**, 108–121.

PEREGRINE, D. H. 1983 Breaking waves on beaches. *Ann. Rev. Fluid Mech.* **15**, 149–178.

PEREGRINE, D. H. 1990 Computations of breaking waves. In *Water Wave Kinematics* (ed. A. Torum and O. T. Gudmestad), pp. 475–490. Kluwer.

PEREGRINE, D. H., COKELET, E. D. & MCIVER, P. 1980 The fluid mechanics of waves approaching breaking. *Proc. 17th Intl Conf. Coastal Engng*, pp. 521–528.

PICKERING, C. J. D. & HALLIWELL, N. A. 1984 Speckle photography in fluid flows: signal recovery with two step processing. *Appl. Optics* **23**, 1128–1129.

QUINN, P. A., SKYNER, D. J., GRAY C., GREATED, C. A. & EASSON, W. J. 1992 A critical analysis of the particle image velocimetry technique as applied to water waves. *Flow Visualization and Image Analysis* (ed. F. T. M. Nieuwstadt). Kluwer.

SALTER S.H. 1982 Absorbing wave makers and wide tanks. *Proc. Conf. Directional Wave Spectra Applications*, pp. 185–200. ASCE.

SAND, S. E., HANSEN, N. E. O., KLINTING, P., GUDMESTAD, O. T. & STERNDORFF, M. J. 1990 Freak wave kinematics. In *Water Wave Kinematics* (ed. A. Torum & O. T. Gudmestad), pp. 535–549. Kluwer.

SHE, K., GREATED, C. A. & EASSON, W. J. 1992 Development of a two-dimensional numerical wave tank. *Proc. 2nd Intl Conf. Offshore Polar Engng*, vol. 3, pp. 102–113.

SIMPKINS, P. G. & DUDDERAR, T. D. 1978 Laser speckle measurement of transient benard convection. *J. Fluid Mech.* **89**, 665–671.

SKYNER, D. J. 1992 The mechanics of extreme water waves. PhD thesis, the University of Edinburgh.

SKYNER, D. J. & GREATED, C. A. 1992 The evolution of a long-crested deep-water breaking wave. *Proc. 2nd Intl Conf. Offshore Polar Engng*, vol. 3, pp. 132–138.

SKYNER, D. J., GRAY, C. & GREATED, C. A. 1990 A comparison of time-stepping numerical predictions with whole-field measurements in breaking waves. In *Water Wave Kinematics* (ed. A. Torum & O. T. Gudmestad), pp. 491–508. Kluwer

SUTHERLAND, J., GREATED, C. A. & EASSON, W. J. 1991 Crest kinematics in wave groups. *Proc. 1st Intl Conf. Offshore Polar Engng*, vol. 3, pp. 97–103.

TALLENT, J.R., YAMASHITA, T. & TSUCHIYA, Y. 1990. Transformation characteristics of breaking water waves. *Water Wave Kinematics* (ed. A. Torum & O. T. Gudmestad), pp. 509–523. Kluwer.